Cell, Vol. 96, 131–141, January 8, 1999, Copyright ©1999 by Cell Press

Structure of CheA, a Signal-Transducing Histidine Kinase

Alexandrine M. Bilwes,* Lisa A. Alex,* Brian R. Crane,† and Melvin I. Simon*‡
*Department of Biology
†Department of Chemistry
California Institute of Technology
Pasadena, California 91125

Summary

Histidine kinases allow bacteria, plants, and fungi to sense and respond to their environment. The 2.6 Å resolution crystal structure of *Thermotoga maritima* CheA (290-671) histidine kinase reveals a dimer where the functions of dimerization, ATP binding, and regulation are segregated into domains. The kinase domain is unlike Ser/Thr/Tyr kinases but resembles two ATPases, Gyrase B and Hsp90. Structural analogies within this superfamily suggest that the P1 domain of CheA provides the nucleophilic histidine and activating glutamate for phosphotransfer. The regulatory domain, which binds the homologous receptor-coupling protein CheW, topologically resembles two SH3 domains and provides different protein recognition surfaces at each end. The dimerization domain forms a central four-helix bundle about which the kinase and regulatory domains pivot on conserved hinges to modulate transphosphorylation. Different subunit conformations suggest that relative domain motions link receptor response to kinase activity.

Introduction

Signal-transducing circuits mediated by histidine kinases play a central role in information processing. These circuits are sometimes referred to as "two component systems" or "phosphorelays," and they regulate a large variety of cellular responses, including bacterial chemotaxis, osmoregulation, photosensitivity, sporulation, plant response to ethylene, and microbial pathogenesis (for a review, see Parkinson and Kofoid, 1992; Appleby et al., 1996). The signaling system is generally made up of two or more multidomain proteins (Kofoid and Parkinson, 1988). One component contains a histidine kinase and is linked to a sensory unit that responds to changes in physical conditions by modulating kinase activity. Most histidine kinases are homodimers that use ATP to transphosphorylate a specific substrate histidine residue on the adjacent subunit within the dimer (Yang and Inouye, 1991; Swanson et al., 1993a). The phosphoryl group is then transferred from histidine to a specific aspartyl residue on a response-regulator domain (second component) that may be a separate protein or attached to the histidine kinase. The response regulator, when phosphorylated, acts directly to modify an effector, leading to a change in cellular behavior. These systems are tuned to operate over a wide range of stimuli with time constants extending from 100 ms to hours. Their different functional characteristics are clearly determined by the protein structure of each domain and the arrangement of the various protein domains within each molecule. How various transient associations between components in these complex proteins transfer information largely remains unclear. While three-dimensional structures of several response regulator modules have been obtained, the atomic structure for the complete histidine kinase molecule has been elusive.

A well-studied signaling pathway that uses a two-component system is bacterial chemotaxis. Most bacteria are able to swim by virtue of rotation of their helical flagella. When the flagellar bundle rotates counterclockwise, the bacterium swims smoothly. Switching to clockwise rotation results in a reorientation (tumbling) of the bacterium. Thus, translocation depends upon the frequency of changes in the direction of flagellar rotation. The signaling circuit that controls switching consists of transmembrane chemoreceptors that through an adaptor protein, CheW, regulate the histidine autophosphorylation of the multidomain CheA protein. CheY obtains the phosphate from CheA and becomes the signal to change the direction of flagellar rotation.

Hundreds of different genes can be identified as histidine kinases on the basis of five regions (boxes) of amino acid sequence similarity (Parkinson and Kofoid, 1992; Alex and Simon, 1994; Swanson et al., 1994). We can separate them into two major classes when considering the position in the sequence of the substrate histidine and surrounding residues (H box) with respect to the ATP-binding domain. The ATP-binding domain is delineated by four regions of sequence similarity (N, G1, F, and G2 boxes; Figure 1). In class I histidine kinases, the H box is directly adjacent in sequence to the ATP-binding domain. In the second class of histidine kinases (Figure 1), which is exemplified by CheA, the histidine residue that becomes phosphorylated is located in the P1 domain, a distant separate domain at the N terminus of the protein. The *E. coli* P1 domain is composed of a five-helix bundle with the substrate histidine accessible to solvent on the outer surface of the second helix (Zhou et al., 1995). The P2 domain is inserted between the P1 and the kinase domain and connected by two flexible linkers. P2 is a specific recognition domain for the response regulator CheY, which dephosphorylates P1 (Figure 1) and retains the phosphate on its active site aspartate. The crystal structure of P2 in complex with CheY has been determined (McEvoy et al., 1998; Welch et al., 1998). Here we report the structure of *Thermatoga maritima* CheA that contains the remaining kinase, dimerization, and regulatory modules yet to be structurally characterized for histidine kinases. The dimerization and regulatory modules of CheA are also essential for signal transduction (Morrison and Parkinson, 1997). The regulatory domain specifically binds the adaptor protein CheW to connect the transmembrane chemosensors to CheA, while dimerization is critical for transphosphorylation.

‡To whom correspondence should be addressed (e-mail: simonm@cco.caltech.edu).

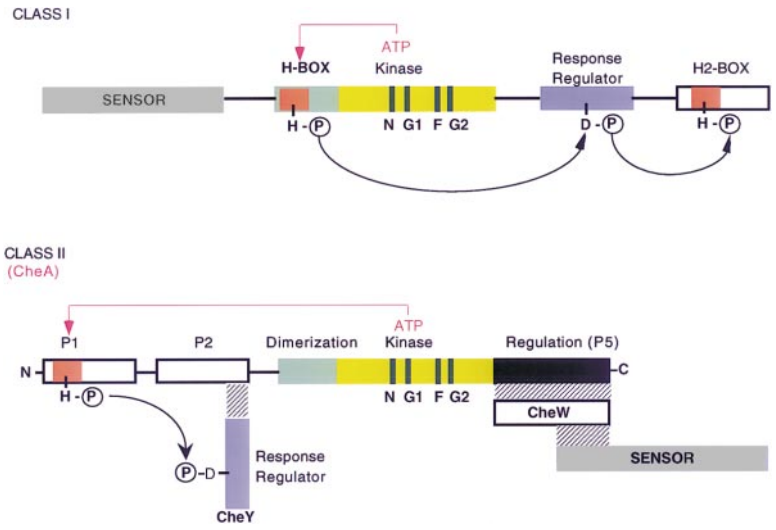

Figure 1. Two Classes of Histidine Kinases

Generalized schematic diagram dividing histidine kinases into two classes based on the position in the sequence of the substrate histidine (H box) with respect to the kinase domain. H, N, G1, F, and G2 boxes are conserved sequence motifs among histidine kinases (Alex and Simon, 1994). Arrows represent the flow of phosphate through these systems. CheW is the coupling protein that interacts (hashed lines) with the sensor (receptor) and CheA.

Results

Structure Determination

Previous attempts to crystallize CheA from *E. coli* failed, so we turned to the homologous CheA from *T. maritima* (Swanson et al., 1996). This organism grows at high temperatures and has a chemotaxis system that is similar to that found in mesophilic bacteria. We recombinantly expressed CheAΔ289 (residues 290–671), which lacks the two amino terminal domains P1 and P2. CheAΔ289 phosphorylates the fragment composed of *T. maritima* P1 and P2 in vitro, and the efficiency of phosphorylation is enhanced by increasing temperature up to 80° (data not shown). In solution, CheAΔ289 forms a complex with recombinant *T. maritima* CheW, and the two proteins copurify. Thus, CheAΔ289 is enzymatically active and retains substrate specificity and binding to CheW.

We determined the crystal structure of CheAΔ289 (residues 290–671) at 2.6 Å resolution by combining experimental phases from multiple isomorphous replacement (MIR) with phases from multiwavelength anomalous diffraction (MAD). Dimeric recombinant wild-type CheAΔ289 and mercury-modified mutants Q545C and E387C produced crystals suitable for structure determination (Tables 1 and 2). Crystals of mercury-modified Q545C diffracted better than wild-type CheAΔ289 and were highly isomorphous with unmodified Q545C (Table 2). Anomalous diffraction from seleno-methionine-containing protein crystals was used to locate 20 methionines in the electron density map and aided the definition of the noncrystallographic symmetry and the tracing of the model. Cycles of model-weighted phase combination, manual rebuilding with interactive graphics, and reciprocal space refinement produced the final structure. Our 2.6 Å resolution refined model of mercury-modified CheAΔ289 Q545C (R factor of 21.3%; R_{free} 28.5%) includes a nonsymmetric dimer of residues 293–671, two mercury atoms, 221 water molecules, and displays reasonable geometry (see Experimental Procedures).

Modular Structure of CheAΔ289

Each CheAΔ289 subunit is a modular protein comprised of three distinct domains linked by hinges at residues Arg-354 and Thr-540 (Figure 2). Each domain embodies a different functionality: dimerization (residues 290–

Table 1. Native and Derivative Data Statistics. 545Hg, Hg3, Hg4 Represent Different Data Sets of CheAΔ289 Q545C Soaked in $HgCl_2$; 387Hg Represents CheAΔ289 E387C Cocrystallized with EMTS; and Seleno 545 Represents Selenomethionine CheAΔ289 Q545C. The Crystal Hg4 Was Used for the Collection of MAD Data.

					Reflections			
Data Set	Resolution[a] (Å)	R_{sym}[b] (%)	I/σ(I)[c]	Completeness (%)	Unique	Observed	Wavelength (Å)	Sites
545Hg	2.6 (2.7–2.6)	6.8 (34.4)	21.2 (3.2)	92.6 (79.5)	33278	93352	1.08	2
545	2.5 (2.6–2.5)	3.9 (28.9)	16.9 (2.9)	78.5 (67.5)	31655	57757	1.08	2
387Hg	3.2 (3.3–3.2)	5.4 (26.9)	17.2 (4.8)	84.4 (78.0)	16572	31820	1.08	2
Hg3	2.7 (2.8–2.7)	6.1 (31.6)	25.4 (7.6)	93.8 (97.1)	31863	170975	0.946	2
Seleno 545	2.5 (2.6–2.5)	6.2 (29.6)	37.2 (8.5)	98.2 (98.9)	40131	196467	0.979	20
Hg4 peak	2.7 (2.8–2.7)	3.9 (30.7)	19.4 (5.7)	93.2 (95.1)	29593	76121	1.001	2
Hg4 inflection	2.6 (2.7–2.6)	5.8 (28.3)	18.5 (5.0)	92.5 (95.7)	32719	80860	0.999	2
Hg4 high remote	2.7 (2.8–2.7)	5.5 (29.1)	17.9 (5.5)	92.8 (95.0)	29847	73990	0.946	2

The first three data sets were collected at SSRL beamline 7-1 on a 30 cm Mar Research Image plate detector; the others were collected at ALS beamline 5.0.2 on a CCD quantum detector.

[a] Highest resolution of data set followed by resolution range in highest bin for compiling statistics.

[b] $R_{sym} = \Sigma\Sigma j|Ij - \langle I\rangle|/\Sigma\langle I\rangle$, I = intensity.

[c] I/σ (I) = signal to noise.

Table 2. MIR & MAD Phasing Statistics. MIR Statistics Are Calculated with 545Hg as the Reference Data Set.

	Resolution (Å)	Phasing Power iso[a]	Phasing Power ano[b]	R*iso* (%)	R*cen* (%)	R*k* (%)	Anomalous Ratio	Dispersive Ratio (Vs Inflection)	Figure of Merit (2.8 Å)
545	2.8	2.18		15.8	52.2				
387Hg	3.5	1.03	0.87	39.2	69.3	50.7	4.6		MIRAS
Hg3	2.8		2.30	15.0		16.6	4.8		0.56
545Hg anomalous	3.5		1.59			17.2	4.3		
Hg4 inflection	2.8						4.1		MAD
Hg4 peak	2.8						4.9	9.8	0.47
Hg4 high remote	2.8						5.1	10.6	
Combined	2.8								0.67

R*k* = $\Sigma||F_{PH}^{+}| - |F_{PH_{calc}}^{+}|| + ||F_{PH}^{-}| - |F_{PH_{calc}}^{-}|| / |F_{PH}^{+}| + |F_{PH}^{-}|$ for anomalous scattering.
Anomalous ratio = rms $||F^{+}| - |F^{-}||$/rms F. Dispersive ratio = rms$||F_{\lambda 1}| - |F_{\lambda 2}||$/rms F, rms = root mean square.
See Table 1 for data set nomenclature.
[a] Phasing power iso = $<|F_H|>/<E>$ where $|F_H|$ is the calculated heavy atom structure factor amplitude and *E* is the lack of closure error.
[b] Phasing power ano = $<2|F_H''|>/<E>$ where $|F_H''|$ is the anomalous correction component amplitude. R*iso* = $\Sigma\Sigma_j||F_j| - <|F|>|/\Sigma<|F|>$.
R*cen* = $\Sigma||F_{PH}| - |F_P| - |F_H||/\Sigma||F_{PH}| - |F_P||$ for centric reflections of isomorphous derivatives.

354), kinase activity (residues 355–540), and regulatory coupling (residues 541–671) (Figure 1). In the overall CheAΔ289 dimer structure, the two kinase and regulatory domains are arranged around a central four-helix bundle in a three-dimensional "X" pattern of dimension $55 \times 120 \times 70$ Å^3 (Figures 2 and 3). There are no contacts between the two regulatory domains or between the two kinase domains. This organization places the two ATP-binding pockets 90 Å apart and rules out functional interaction between the two kinase domains. The internal symmetry within the CheAΔ289 dimer is irregular (Figures 2 and 3, and see later section). Nonsymmetric conformation of the hinge residues Arg-354 and Thr-540, which link the dimerization domain to the kinase domain and the kinase domain to the regulatory domain, respectively, generate different interdomain contacts and relative domain arrangements within the two subunits.

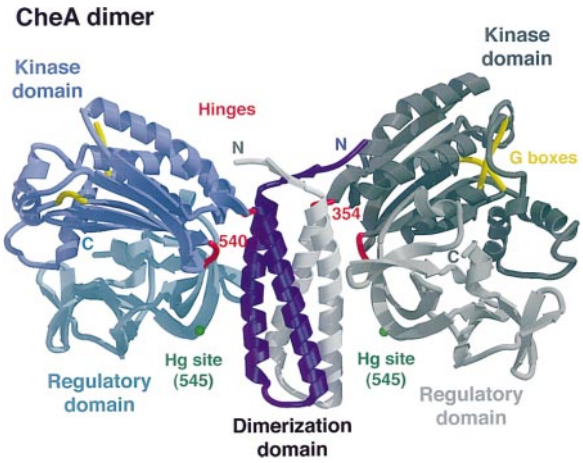

Figure 2. Overall Structure of the CheAΔ289 Dimer

The two subunits (blue for MOL1, gray for MOL2) of the CheA dimer (shown as ribbon diagram) each contain separate dimerization, kinase, and regulatory domains. The dimer associates by a central four-helix bundle and places the 2 ATP-binding sites (located by the G boxes) 90 Å away from each other.

The dimerization domain is dominated by two antiparallel helices (α1, α2) that pack against the analogous two helices of the second subunit to form the central four-helix bundle (Figure 2). The second domain, which contains the kinase activity (Swanson et al., 1993b), is a two-layered α-β sandwich (CATH classification; Orengo et al., 1997) made of a flat, mixed, five-stranded β sheet and six α helices (Figures 2 and 4A). This structure forms a deep cavity presumed to be the ATP-binding site (Figure 5). Three of the helices (α3, α4, α8) are amphipathic and pack parallel to the sheet, whereas the three shorter remaining helices point into the solvent with two (α6, α7) adjacent to the ATP-binding site. The third domain (541–671) regulates the kinase activity by interacting with an activating receptor through the adaptor protein CheW (Bourret et al., 1993). This domain displays two twisted five-stranded β barrels with an unusual topology resulting in two adjacent strands being parallel in each barrel (Figure 6A).

Histidine Kinases Belong to a Superfamily of ATPases

The catalytic domain of the histidine kinase has a completely distinct topology than that of Ser/Thr or Tyr kinases (Figure 4A). However, the kinase domain of CheA shows striking structural similarity (DALI; Holm and Sander, 1993) with two functionally different ATPases (Figure 4): the amino-terminal domain of a type II topoisomerase, Gyrase B (34–211; Brookhaven Protein Data Bank (BPDB) entry code 1aj6; Wigley et al., 1991; Holdgate et al., 1997), and the amino-terminal domain of a chaperone, Hsp90 (39–195 for human Hsp90; BPDB entry codes 1am1, 1yer; Prodromouu et al., 1997; Stebbins et al., 1997). The core structural elements in common between CheA, GyrB, and Hsp90 consist primarily of the four β strands and three α helices that form a deep cavity for binding ATP in GyrB and Hsp90 (Figures 4A and 4B). α3 and β2 in CheA also have equivalents in GyrB and Hsp90, but their topological arrangement differs. In CheA, α3 and β2 precede the core region, whereas in GyrB and Hsp90 they follow the core region (Figures 4A and 4B). Thus, histidine kinases, GyrB, and Hsp90 are

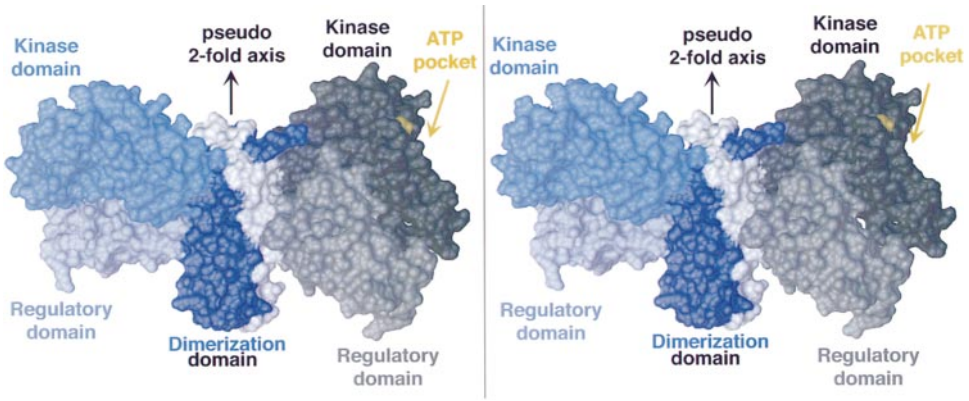

Figure 3. Solvent-Accessible Surface of CheAΔ289

The stereodiagram shows the two subunits (blue for MOL1, gray for MOL2) of the CheA dimer, which place the kinase regulatory domains in a three-dimensional "X" pattern about the central dimer interface. The residues in gold correspond to the two G boxes and identify the ATP-binding pocket.

likely to derive from a common ancestor and have diverged by gene rearrangement.

The ATP-binding residues in GyrB are highly conserved in CheA and thereby allow us to identify CheA's nucleotide-binding cavity. All of the histidine kinase regions of sequence similarity (N, G1, F, and G2 boxes) are found in the kinase domain (Figure 4A), with the exception of the H box containing the substrate histidine, which is found on domain P1 in CheA. The back wall of the cavity that generates the presumed ATP-binding site in CheA is formed by the domain's β sheet elements, while the edges of the site are generated by four homology regions: α4 (N box), a segment running in front of the sheet and following a right angle turn after strand β4 (G1 box), the end of helix α7 (F box), and the beginning of helix α8 with the end of the loop preceding it (G2 box). The back of this pocket is mainly hydrophobic except for highly conserved residues Asp-449, Asn-409, Thr-531, and Ser-525 located at one end of the cavity. In the crystal structure of GyrB in complex with the ATP analog ADPNP (5′-adenylyl-β-γ-imidodiphosphate) (Wigley et al., 1991), the equivalents of CheA Asp-449 (Asp-73) and Thr-531 (Thr-165) hydrogen bond to the adenine amine, whereas the equivalent of CheA Asn-409 (Asn-46) hydrogen bonds to the Mg^{2+} ion, which coordinates the three phosphates of ATP (Figure 4B). These ATP-binding residues and the hydrophobic residues lining the back of the ATP pocket are conserved in all histidine kinases (Figure 4C), including the cyanobacterial phytochrome Cph1 (Yeh et al., 1997). The few differences in residues that bind ATP between GyrB and CheA conserve functionality. For example, in GyrB, Lys-103, preceding the G2 box, binds the ATP β-phosphate, whereas in CheA, conserved His-413, which instead resides on α4, is positioned to provide the same interaction. Mutation of this residue to a Tyr severely curtails autophosphorylation (CheA allele 504 described in Oosawa et al., 1988), consistent with it having a role in ATP binding.

By analogy with GyrB, the CheA G2 loop is likely to dramatically change conformation upon binding the ATP phosphates. The G2 box in GyrB forms a loop whose main chain nitrogen atoms come in close contact with the phosphates of ADPNP. However, in the crystal structure of GyrB bound to the antibiotic novobiocin (Holdgate et al., 1997), the G2 loop is in an extended conformation away from the ATP pocket. The limited order and extended conformation of this loop in our ATP-free CheA structure indicates inherent flexibility and suggests that the G2 loop is likely to change conformation and fold onto bound ATP as well. In summary, the sequence and structural homology between GyrB and CheA allows us to predict the nature of the histidine kinase ATP-binding site. We further predict a large movement of the G2 loop upon ATP binding.

A Probable Mechanism for Histidine Phosphorylation

In contrast to GyrB, which hydrolyses ATP, kinases must transfer phosphate, and therefore the nucleophilic mechanism for attack on the ATP γ-phosphate must differ between the two enzymes. In GyrB, mutagenesis studies (Jackson and Maxwell, 1993) implicate the conserved Glu-42 (corresponding to Glu-47 in human Hsp90; Panaretou et al., 1998) as an essential general base for water activation. Despite high conservation of active site residues between GyrB and histidine kinases (Figure 4C), the latter do not contain a Glu at this position (His-405 for CheA proteins, Gln and Arg for other His kinases). This difference may explain why histidine kinases are not purely ATPases and require external residues for phosphate transfer. An obvious candidate for direct nucleophilic attack on the ATP γ-phosphate in CheA is the phosphate-accepting His-45 in domain P1. In fact, the increased pKa (7.8) of the accepting histidine on the *E. coli* P1 domain (Zhou and Dahlquist, 1997) suggests increased nucleophilicity resulting from its interaction with conserved Glu-67 (Glu-70 in *E. coli*; Zhou and Dahlquist, 1997). Furthermore, mutation of Glu-70 in *E. coli* CheA to a Lys markedly decreased autophosphorylation activity (CheA allele 510 described in Oosawa et al., 1988). Thus, the CheA P1 domain may provide not only the nucleophile for phosphate transfer (His-45) but also the activating glutamate (Glu-67), thereby completing the catalytic center observed in GyrB.

Accessibility of the ATP γ-phosphate to residues from

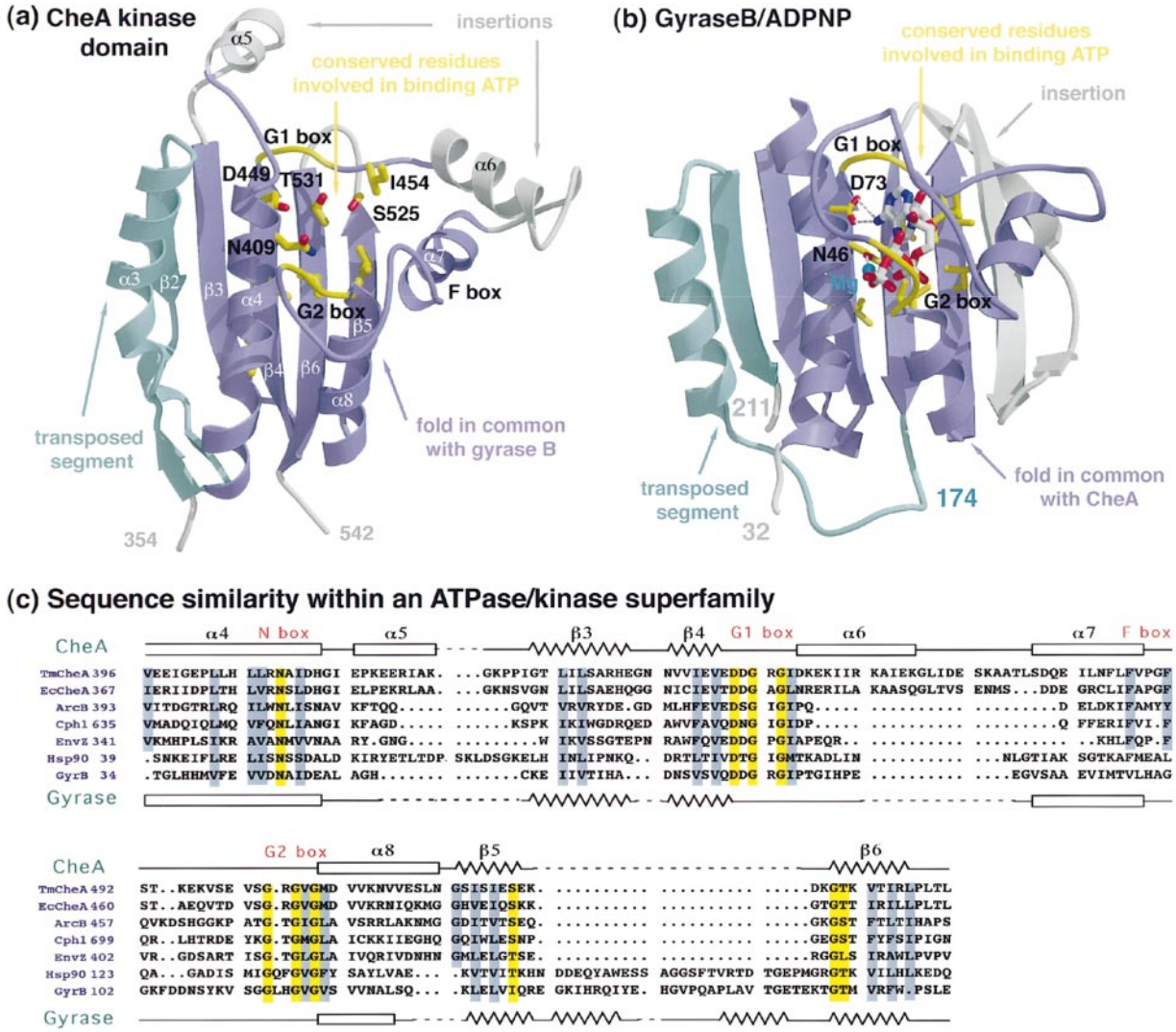

Figure 4. The Kinase Domain of CheA Resembles GyrB

(A and B) The kinase domain is structurally similar to the region spanned by residues 32 to 211 of the amino-terminal domain of Gyrase B, shown with ADPNP (white) bound in its ATP-binding pocket. The topology between domains is the same, except for a transposed segment (turquoise) that is joined to the amino terminus of the core region (mauve) in CheA, whereas it is joined to the carboxy terminus of the core region (mauve) in Gyrase B. The elements of secondary structure that are not shared between the two structures (gray) are away from the ATP-binding site. Additional terminal secondary structure elements in GyrB not in common with CheA are not shown. Many residues lining the ATP-binding site (yellow) are conserved between the two proteins. The rmsd of the Cα positions for the secondary structure elements common between CheA and GyrB is 2.3 Å.

(C) Sequence similarity in an ATPase/kinase superfamily. The boxes of sequence similarity identified for histidine kinases can be aligned with similar sequence signature motifs in GyrB and Hsp90, with the exception of the F box. Conserved hydrophilic residues involved in Mg–ATP binding are shown in gold. Conserved hydrophobic residues (blue) are involved in lining the ATP-binding site or structuring the domain topology (secondary structure: top line for CheA, bottom line for GyrB). The sequences presented in the figure are for *T. maritima* CheA (TmCheA), *E. coli* CheA (EcCheA), *E. coli* ArcB, *Synechocystis sp.* Cph1 , *E. coli* EnvZ , human Hsp90, and *E. coli* Gyrase B (GyrB).

a distinct domain in GyrB (Wigley et al., 1991) suggests that this ATP-binding module is designed to allow access of external residues to the ATP γ-phosphate. In fact, a shallow groove observed in the CheA structure beside the putative position of the ATP γ-phosphate could be a recognition surface for P1 (Figure 5). Given the high sequence conservation between *E. coli* and *T. maritima* CheA P1 in the region immediately surrounding His-45 on helices B and C (Zhou et al., 1995), yet the inability of *T. maritima* CheAΔ289 to phosphorylate an *E. coli* P1–P2 fragment (data not shown), the interface between P1 and the kinase domain is likely to include residues on P1 not immediately surrounding His-45.

A Separate Module Is Exclusively Responsible for Stable Dimerization

The extensive, hydrophobic dimerization interface in CheA creates a large energy barrier for dissociation of the subunits consistent with the dimeric state of CheA in solution (Gegner and Dahlquist, 1991). The dimerization domain accounts for over 97% of the 1600 Å^2 of surface

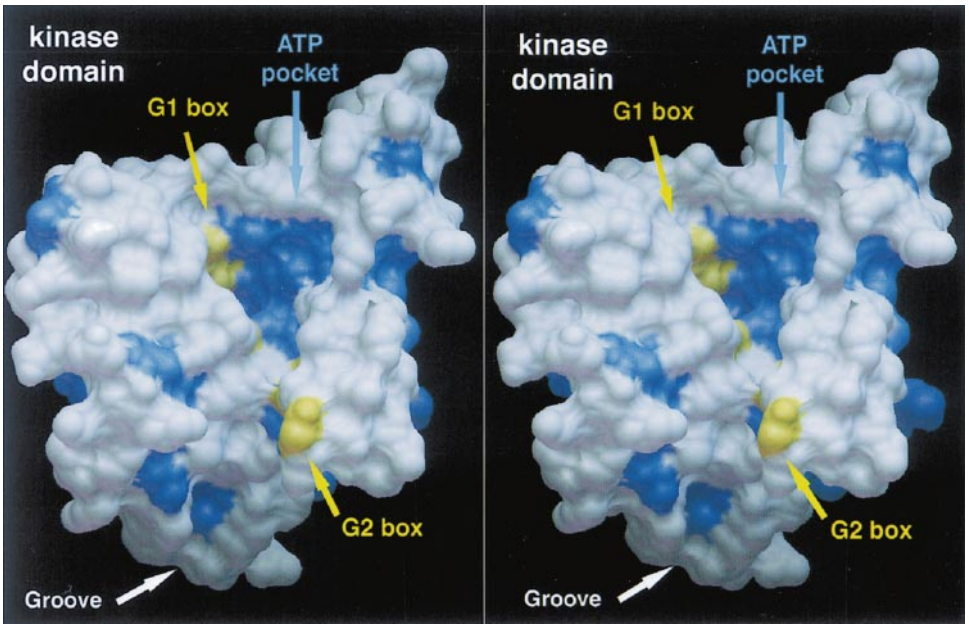

Figure 5. Stereo View of the Solvent-Accessible Surface of the CheA Kinase Domain

The deep ATP-binding pocket is lined by exposed hydrophobic residues that are conserved among histidine kinases (blue). The G1 and G2 boxes (gold) border the cavity. A shallow groove below the G2 box may form a surface for binding of the CheA P1 domain.

area buried on each subunit in the dimer interface (calculated with MS using a 1.4 Å probe radius; Connolly, 1983). The four-helix bundle formed by dimerization has both amino termini on the same end of the bundle and has a left-handed twist. This symmetry allows each helix to be antiparallel to the two adjacent helices, which is the most stable arrangement for a four-helix bundle (Chou et al., 1988). To complete CheA's dimerization domain, a 6-residue long amino-terminal strand interacts with its noncrystallographic equivalent to form an antiparallel two-stranded β sheet, capping the exclusively hydrophobic interface between the four helices. In addition, the two interhelix loops (325–328 in MOL1 and 328–331 in MOL2) protect the other end of the hydrophobic core. As a result, the N terminus of the dimerization domain is likely to direct P2 and P1 toward the symmetry-related kinase domain, consistent with transphosphorylation of P1 (Swanson et al., 1993a). Because the dimerization domain is isolated from the kinase domain and primarily responsible for subunit association in CheAΔ289, maintenance of this module suggests that formation of a stable dimer is critical. Furthermore, the dimerization domain may also be important for regulation of signaling (Morrison and Parkinson, 1997).

Class I histidine kinases (Figure 1) are likely to share a similar dimerization motif with CheA. The region corresponding to the dimerization domain has high sequence conservation within the CheA class but moderate conservation with class I histidine kinases. Yet, an alignment of 26 representative class I sequences around the H box (not shown) displays a periodicity of conserved hydrophobic residues indicative of two amphipathic helices preceding the kinase domain. Furthermore, subdomain A (223–289) preceding the EnvZ histidine kinase domain is the same size as the CheA dimerization domain; it forms a homodimer in solution and is primarily helical by CD spectroscopy (Park et al., 1998). Unlike CheA, this domain contains the target histidine for phosphorylation. Homodimerization of EnvZ subdomain A could produce a four-helix bundle similar to the core region of the CheA P1 domain (Zhou et al., 1995), the Hpt domain (H2 box) of class I histidine kinase ArcB (Kato et al., 1997), and the dimeric H box of the phosphotransferase Spo0B (Varughese et al., 1998). Movement is possible around a hinge region between the dimerization domain and the kinase domain in CheA. A similar hinge in EnvZ-related kinases may allow the kinase domain to transphosphorylate the substrate histidine on the dimerization domain.

A Common Topology for Kinase Regulation

The CheA regulatory domain, termed P5 (Figure 1), has a topology related to that of SH3 domains, modules that regulate kinase activity in higher organisms by mediating transient protein–protein interactions (Schlessinger, 1994). No equivalent of an SH3 domain has been found previously in bacteria. The two β barrels of the regulatory domain are related by pseudo-2-fold symmetry, an observation unexpected from sequence comparison. Unlike typical structures resulting from gene duplication, the two barrels are not traced consecutively (Figure 6A). The chain starts in the first barrel by a β hairpin and then travels into the second barrel to form three consecutive β strands and a hairpin similar to the first. Finally, the chain returns to the first barrel to trace the last three β strands. Thus, the structure can be described as two consecutive β barrels that swap a central β hairpin between them. If the second barrel is considered as an insertion into the first, the first barrel has a topology identified by the similarity search program Dali (Holm and Sander, 1993) as being related to that of an Src-homology-3 (SH3) domain (Figure 6A; Xu et al., 1997).

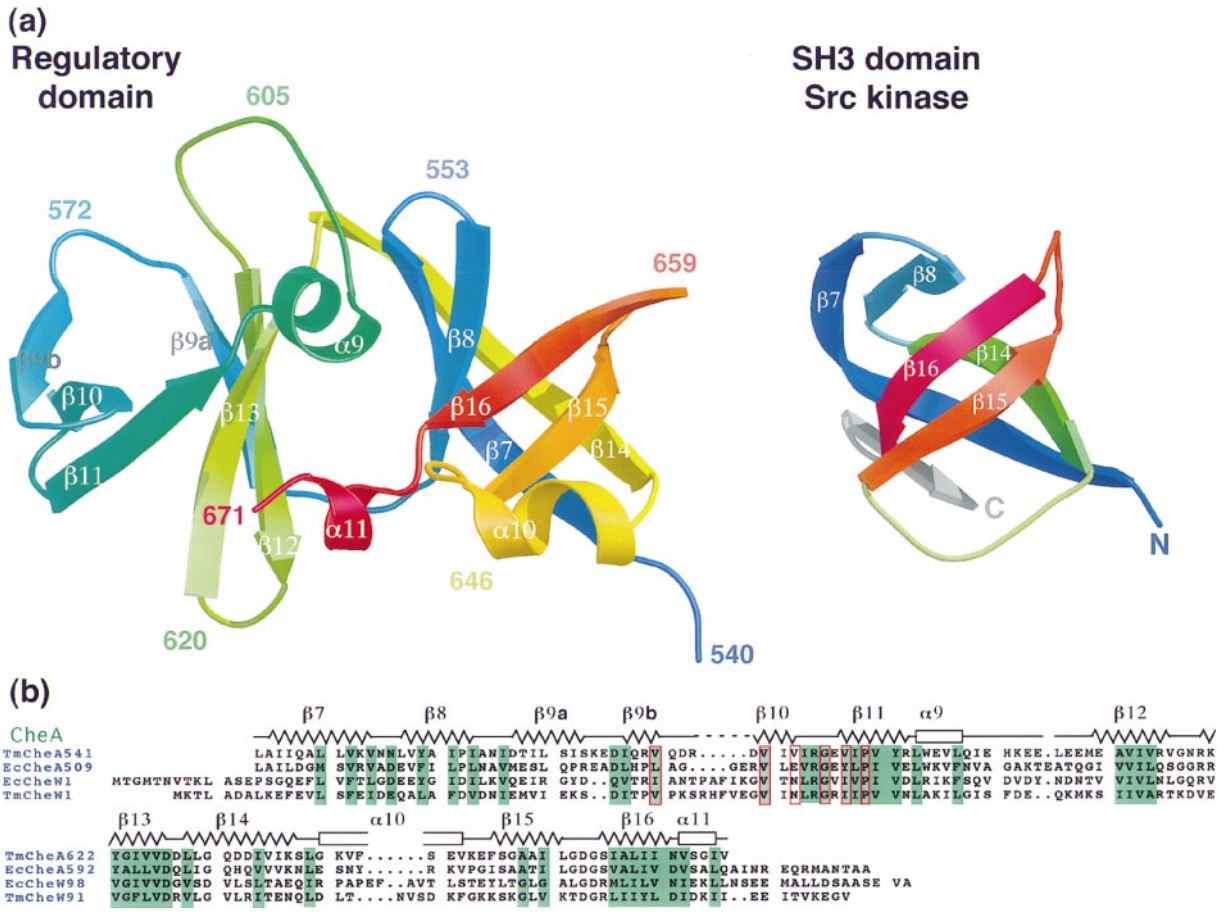

Figure 6. The CheA Regulatory Domain Resembles Two SH3 Domains

(A) The regulatory domain (left, residues 540–671) forms two β barrels that are related by pseudo-2-fold symmetry. Each barrel is topologically related to the SH3 domain of human c-Src kinase (right; Xu et al., 1997). Topologically equivalent β strands between the first CheA barrel (right) and c-Src SH3 have matching labels (CheA assignments) and colors. Each CheA barrel can be viewed as an SH3 domain that swaps its first β hairpin with the opposing barrel, or the second β barrel can be viewed as an insertion into the first between β8 and β14. Superposition of the β strands of c-Src SH3 domain with the β strands of the first CheA barrel gives an rmsd of 1.8 Å for 34 Cα atom positions if β8, which is involved in the connection to the second CheA barrel, is excluded.

(B) The sequences for the regulatory domains of *T. maritima* CheA (TmCheA) and *E. coli* CheA (EcCheA) show significant similarity with the sequences of *E. coli* CheW (EcCheW) and *T. maritima* CheW (TmCheW). The most extensive regions of homology (green) form most of the regulatory domain's β strands, 2 β turns, and the connections between barrels (secondary structure, top line). Moreover, the residues boxed in red participate in an extensive symmetrical contact between two regulatory domains that belong to two different dimers in the CheAΔ289 crystal lattice.

Superimposing the β strands of the first barrel with the β strands of the Src-SH3 domain (BPDB code 1fmk) produces a root-mean-square deviation of 1.8 Å for 34 Cα atoms and reveals a conserved central hydrophobic core (Figure 6A). If the two central β hairpins of the CheA regulatory domain were not swapped between the two barrels, then both barrels would have a topology similar to that of an SH3 domain. Reversible swapping of a different β hairpin between two SH3 domains has been observed in the atypical intertwined SH3 dimer of mouse signal transduction protein Eps8 (Kishan et al., 1997). Similar to the Eps8 SH3 dimer structure, the exclusively hydrophobic interface between β barrels in CheA partially contains the molecular surface that recognizes polypeptides in typical SH3 domains. Thus, the CheA regulatory domain and typical SH3 domains recognize different protein targets with different surfaces. However, the coupling of an SH3-like domain to a histidine kinase mirrors the association of SH3 domains with tyrosine kinases in mammals. Thus, SH3-like domains must constitute malleable scaffolds for the engineering of specific protein or peptide recognition surfaces in bacteria as in other organisms.

The regulatory domain, which mediates the interaction between CheA and CheW (Bourret et al., 1993; Morrison and Parkinson, 1997), is likely to be structurally related to CheW (Figure 6B). A BLAST sequence similarity search (Altchul et al., 1997) with *T. maritima* CheW as a probe identified significant sequence similarity with the regulatory domain of several CheA proteins. For example, *Borrelia burgdoferi* $CheA_2$ (residues 767–757) and *T. maritima* CheW (residues 52–143) gave the highest similarity score (BLAST expect value 4×10^{-4}) with 28% identity over 97 residues. Given the extent of the sequence identity for the length of the alignment, the two proteins can be expected to be structurally related

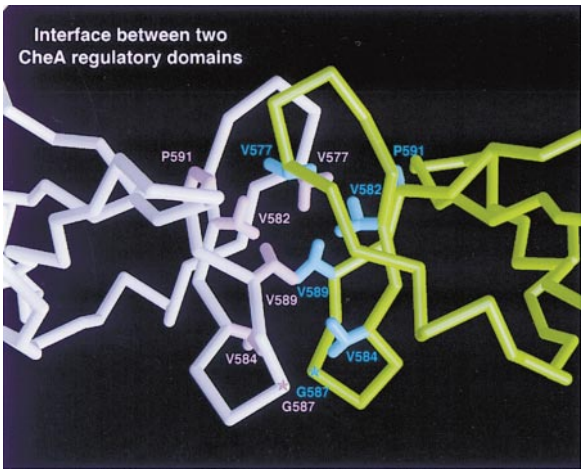

Figure 7. A Possible Interface between CheA and CheW

An extensive interface between two regulatory domains (white, green) that belong to two different dimers has residues conserved by both CheA and CheW (see Figure 6B). Hydrophobic side chains (pink, blue) dominate the interface.

(Sander and Schneider, 1991; Eisenhaber et al., 1995). Moreover, a multialignment of six CheA regulatory domain sequences and ten CheW sequences identifies four regions of high similarity that form important structural elements in the regulatory domain (Figure 6). One region that contains invariant residues Val-626, Asp-627 forms the kink connecting β13 to β14 between the two barrels. The most extensive region of sequence similarity contains invariant residues Val-582, Arg-586, Gly-587, Pro-591 and corresponds to β10 and β11. This region forms an exposed hydrophobic face of the regulatory domain that is most peripheral to the dimerization domain and is involved in an extensive contact with a symmetry-related regulatory domain in the CheAΔ289 crystal lattice (Figure 7). This contact may represent a functional interface between CheA and CheW. Evolving such an interface in a homodimer that was the progenitor of both CheW and the regulatory domain would allow the gain from dimer-stabilizing mutations to be doubled by symmetry.

Flexibility of Interdomain Contacts May Be Important for Signaling

Limited interactions between the dimerization and kinase domains, differences in their relative positioning within each subunit of the dimer, and conserved hinge regions indicate that the relative movement of these domains is likely an essential feature of signaling by multidomain histidine kinases. In one subunit, the interaction between the kinase and dimerization domains is dominated by a salt bridge involving conserved hinge residue Arg-354 and conserved kinase residue Asp-392. In the other subunit, the relative positioning of the domains is different, and the Arg-354 salt bridge is replaced by one between Lys-352 and Glu-390. The two subunit arrangements in the crystal may represent two different favorable arrangements allowed by movement about this hinge (Figure 8). Mutation of the hinge residue Arg-354 to Cys in *E. coli* CheA diminishes autophosphorylation and suppresses chemotaxis (CheA allele 540 described in Oosawa et al., 1988), suggesting that residues that affect domain arrangements are critical for activity and signaling. In the case of class I histidine kinases, such a hinge would have to allow the kinase domain to reach the substrate domain on the dimer interface and then release it for subsequent transfer of the phosphate from the H box to a response regulator domain.

Domain motion about hinges may also allow regulation of kinase activity by the chemoreceptor and CheW. In our structure, P5 could interfere with P1 binding to the kinase in only one subunit (Figures 2 and 8). In this subunit, α10 of P5 resides between α4 and α8 in the kinase domain, near the shallow groove where P1 is presumed to access the ATP γ-phosphate (Figures 4A, 5, and 8). In the other subunit, a rigid body rotation of P5 about a hinge at Thr-540 produces a more open conformation with α10 alongside the C-terminal end of α8 (Figure 8). Both the closed and open conformations are stabilized by a salt bridge between Glu-398 and Lys-642, but the Cα atoms of these residues are 6 Å closer in the closed conformation. The two different domain arrangements also manifest a 25° scissors movement between the regulatory and dimerization domains (Figure 8). These two domains pivot about a conserved interface involving invariant residues Ile-315 and Gly-311 on α1 and Ile-543 and Val-636 on β7 and β14. The inequivalency between subunits in the dimer allows only one of the regulatory domains to participate in the dimer interface by contacting the second helix of the symmetry-related dimerization domain. Movement within the receptor due to changes in ligand occupancy may be propagated through CheW to P5. Thus, P5 may act as a gatekeeper for P1 access to the ATP-binding site by changing its orientation relative to the dimerization domain, the kinase domain, and CheW. The P5 regulatory domain was divided into two subdomains, M and C, based on the phenotypes of missense mutants (Parkinson and Kofoid, 1992; Morrison and Parkinson, 1997). These domains may correspond to each β barrel of P5 with the most peripheral interacting with CheW and the other binding the dimerization and kinase domains.

Modularity for Signal Transduction and the Coupling of Molecular Motion to ATP Hydrolysis

It has long been recognized that modular organization is critical to signal transduction in the histidine kinases (Hess et al., 1988; Kofoid and Parkinson, 1988; Parkinson and Kofoid, 1992). Signal transduction via tyrosine kinases in higher organisms is also characterized by the modular organization of its components, and the general strategy embodied in the structure of these divergent systems is similar. Consistent with the analogy to the Tyr-kinase signaling pathways, we find CheA histidine kinases linked to a domain reminiscent of an SH3 domain. As with typical SH3 domains, the CheA regulatory domain and homologous CheW are involved in regulation by protein/protein interactions. Also, analogous to SH3 domains, P5-type domains are found as separate

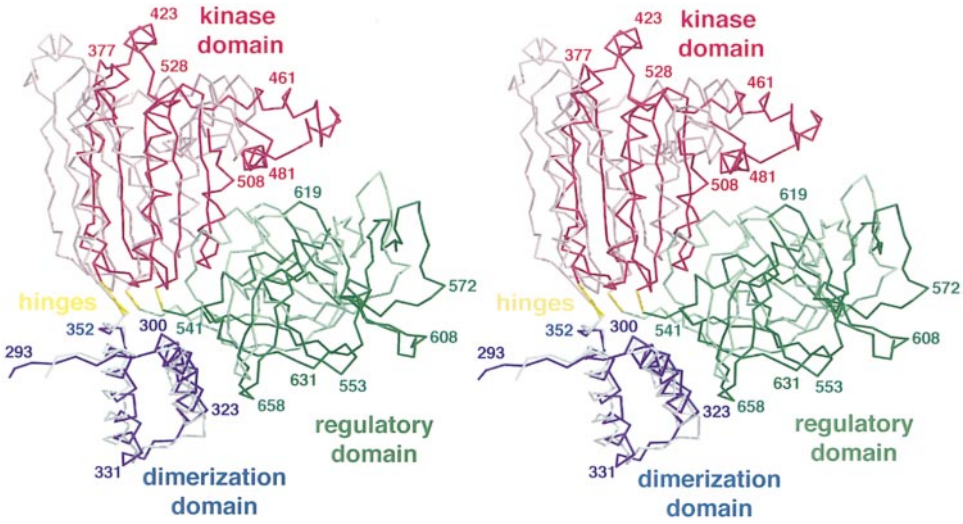

Figure 8. Mobility about Hinges Indicated by Different Subunit Conformations

The two subunits that form the dimer (dark colors for MOL1, light for MOL2) in the asymmetric unit are not superimposable. The positioning of MOL1 onto MOL2 was generated after least-square superposition of the Cα from the dimerization domain only. Different positioning of each domain with respect to its neighbors in the asymmetric unit results from rotation around the conserved hinges (yellow) at residues 354 and 540. As a result, interfaces between domains differ in the two subunits. In the more closed conformation (light, MOL2), α10 from the regulatory domain interacts with the kinase domain near the proposed position of the γ-phosphate (center), possibly interfering with the association of the CheA domain P1.

modules within multidomain proteins of varying functionality, for example, a kinase (CheA), a response regulator (CheV; Fredrick and Helmann, 1994), or an adaptor protein (CheW). The function of dimerization in CheA is also confined to a separate module that links the kinase domain to another CheA molecule but still allows relative domain motions.

CheA shows striking topological similarity with the phosphotransferase Spo0B. Spo0B mediates the transfer of phosphate between the response regulator Spo0F and the transcription factor Spo0A during initiation of sporulation in *Bacillus subtilis* (Burbulys et al., 1991). Spo0B (Varughese et al., 1998) is a dimer composed of a central four-helix bundle and two C-terminal α/β domains topologically related to the ATP-binding domain of CheA. However, this kinase-like domain in Spo0B is much shorter than the kinase domain in CheA and lacks all of the residues involved in binding ATP. Thus, the C-terminal domain in Spo0B is not likely to bind ATP and instead functions only to mediate interaction with other components of this signaling pathway. Moreover, the dimerization domain in Spo0B also contains an H box and is therefore more analogous to class I histidine kinases (Figure 1). The topological similarity between CheA and Spo0B shows that signal transduction circuits in bacteria have derived different functions from similar structural modules.

Finally, the structural similarity among the histidine kinases, type II topoisomerases, and Hsp90 protein chaperones suggest a common mechanism linking ATP hydrolysis to relative subunit motion. Histidine kinases must use conformational motion for coupling extracellular signals to histidine phosphorylation, while GyrB couples ATP hydrolysis to subunit dissociation and the release of relaxed DNA (Bates and Maxwell, 1997). The large amplitude molecular motions common to these events likely involve movements of the kinase or ATPase domain relative to other domains or subunits in these molecules. The structure of CheAΔ289 is a clear example of a molecular architecture in which the arrangement of separate catalytic, substrate, organizing, and regulatory modules can influence and respond to kinase activity through conserved hinge regions and adaptable interfaces. The crystal structure provides an opportunity to explore the details of these interactions. Furthermore, since circuits including histidine kinases have thus far been found only in plants, fungi, and bacteria, and not in mammalian organisms, they represent excellent targets for antibiotics, herbicides, and fungicides. The atomic structure of these complex transducers provides a focus for drug design.

Experimental Procedures

Protein Cloning and Preparation

T. maritima CheAΔ289 (290–671) was subcloned in the vector pET28(a) (Novagen) by PCR between the NdeI and BamHI restriction sites, which placed a His_6 tag at the amino terminus of the protein. Mutations I521M and S522G in CheAΔ289 (introduced by PCR cloning) do not affect kinase activity or binding to CheW, but yield better-diffracting crystals. Eleven different cysteine mutants were constructed by Quickchange mutagenesis (Stratagene) for derivatization with heavy atoms. About 50 mg of recombinant CheAΔ289 was obtained from a 2 L culture of *E. coli* strain BL21(DE3) (Novagen) transformed with our plasmid. The *E. coli* methionine auxotroph strain B834(DE3) (Novagen) was used for expressing seleno-methionine-containing protein. CheAΔ289 was purified in three steps: affinity chromatography on Nickel-NTA beads (Qiagen), overnight thrombin digestion of the His_6 tag at 4°C, and gel filtration on a superdex 200 column (Pharmacia). Protein was concentrated to near saturation (~20–80 mg/ml, depending on the mutant) by centrifugation (with an Amicon centriprep 30 concentrator) in 50 mM Tris (pH 7.5),

150 mM NaCl (+10 mM DTT for the seleno-methionine-containing protein).

Crystallization and Data Collection

Crystals grew by vapor diffusion against a reservoir of 80 mM succinate (pH 5.5), 20% MPD, 5% isopropanol, 3%–7% PEG 8000 in several days at room temperature. Liquid nitrogen–cooled crystals belong to the space group $P2_1$ (a = 61.8 Å, b = 126.5 Å, c = 75.1 Å, $\beta = 95.6°$) and contain one CheA dimer per asymmetric unit (V_M = 3.5 Å^3/Da, solvent content = 65%). Mutant Q545C crystals were soaked for 20 hr in 30% saturated $HgCl_2$ in crystallization buffer. Mutant E387C-Hg crystals grew after preincubation of the protein with 4 mM EMTS (ethyl mercurythiosalicylate) for 4 hr at pH 7.5. Derivatives were identified from diffraction data collected at SSRL beamline 7-1 on a 30 cm Mar Research Image plate detector, and MAD data was collected at ALS beamline 5.0.2 on a CCD Quantum detector. Data was processed by DENZO/SCALEPACK (Otwinowski and Minor, 1997).

MIR and MAD Analysis, Model Building, and Refinement

Mercury atoms positions of derivatized CheA were determined by Patterson map analysis (XTALVIEW; McRee, 1992). Phases derived from MIR (PHASES; Furey and Swaminathan, 1997) and MAD (MADPHSREF; Crane and Getzoff, 1997) were combined (MADPHSREF) and solvent flattened (DM; Collaborative Computational Project, 1994) to produce the first interpretable electron density map at 2.8 Å resolution (Table 2). All native 20 methionines positions were identified from Bijvoet difference Fourier maps of seleno-methionine-modified crystals calculated with solvent-flattened experimental phases. Noncrystallographic symmetry matrices for the three separate CheA domains were determined by comparing Hg sites, Se sites, and fragments of interpreted secondary structure. Each domain superimposes with its noncrystallographic equivalent to give rmsd of 1.7 Å, 0.7 Å, and 1.1 Å for the Cα positions of the dimerization, kinase, and regulatory domains respectively. The three domains are individually related to each other by different symmetry (polar angles ϕ, ψ, κ and translation vectors Tx, Ty, Tz for the dimerization domain = 98°, 136°, 182°, 41.3 Å, −6.9 Å, −41.8 Å; the kinase domain = 89°, 143°, 157°, 29.6 Å, −3.6 Å, −38.0 Å; and the regulatory domain = 107°, 138°, 166°, 39.5 Å, −26.9 Å, −35.6 Å). Note that polar κ angles around these pseudo-2-fold axes differ considerably. Density modification and noncrystallographic averaging (DM) produced an electron density map of sufficient quality to build the initial model. Cycles of manual rebuilding (XFIT; McRee, 1992), partial model phase combination (SIGMAA; Read, 1986), resolution extension to 2.6 Å, and reciprocal space refinement (XPLOR version 3.8; Brünger, 1991) produced the final model (R factor of 21.3% [31.0%]; R_{free} 28.5% [31.8%] for data from 20.0 to 2.6 Å [2.72–2.60 Å]). Due to the inequivalencies between subunits, noncrystallographic symmetry restraints were applied to only 40% of the main chain atoms (rmsd for restrained atoms = 0.18 Å). High solvent content and anisotropic diffraction was corrected in XPLOR with the bulk solvent correction and an overall anisotropic temperature factor (B11 = 18.9 Å^2, B22 = 7.9 Å^2, B33 = 0.4 Å^2, B13 = 13.1 Å^2, when scaling F_{calc} to F_{obs}). The model has reasonable geometry (rmsd bonds = 0.009 Å, rmsd angles = 1.6°) with 87% of all residues having the most favored backbone ϕ, ψ angles, and no residues having disallowed ϕ, ψ angles, as defined by PROCHECK (Laskowski et al., 1993). Refined overall temperature factors of 60.3 Å^2 (58.0 Å^2 for main chain atoms, 61.0 Å^2 for side chain atoms, and 61.9 Å^2 for water molecules) are consistent with the 62.8 Å^2 overall thermal factor obtained from Wilson scaling of the diffraction data (CCP4). Regions 493–503 in MOL1 and 602–609 in MOL2 are disordered; the equivalent regions in the opposite subunit are not well ordered.

Sequence Searches and Alignments

Sequence similarity searches were done with BLAST (Altschul et al., 1997). Sequence alignments were produced with Pileup and adjusted manually if necessary with Lineup (Sequence Analysis Software Package of the Genetics Computer Group; Madison, WI).

Computer Graphics

Figures 2, 4A, 4B, 6A, and 8 were produced with MOLSCRIPT (Kraulis, 1991) and RASTER3D (Merritt and Murphy, 1994). Figures 3 and 5 were rendered in AVS (Advanced Visualization Systems Inc., Waltham, MA). Figure 7 was produced with XFIT and RASTER3D.

Acknowledgments

The authors wish to thank D. C. Rees, P. J. Bjorkman, C. Starks, J. P. Noel, the Stanford Synchrotron Radiation Laboratory (Palo Alto), and the Advanced Light Source (Berkeley; T. Earnest and his coworkers) for access to X-ray diffraction facilities; D. B. Wigley for making the undeposited coordinates of GyrB complexed with ADPNP available to us; and D. C. Rees, P. J. Bjorkman, T-M. Yi, J. Wilker, and H. Li for helpful discussion and critical reading of the manuscript. This work is supported by NIH grant AI19296 and a Donald E. and Delia B. Baxter Foundation Fellowship to A. M. B.

Received October 13, 1998; revised November 23, 1998.

References

Alex, L.A., and Simon, M.I. (1994). Protein histidine kinases and signal transduction in prokaryotes and eukaryotes. Trends Genet. *10*, 133–138.

Altschul, S.F., Madden, T.L., Schaffer, A.A., Zhang, J., Zhang, Z., Miller, W., and Lipman, W. (1997). Gapped BLAST and PSI-BLAST: a new generation of protein database search program. Nucleic Acids Res. *25*, 3389–3402.

Appleby, J.L., Parkinson, J.S., and Bourret, R.B. (1996). Signal transduction via the multi-step phosphorelay: not necessarily a road less traveled. Cell *86*, 845–848.

Bates, A.D., and Maxwell, A. (1997). DNA topology: Topoisomerases keep it simple. Current Biol. *7*, R778–R781.

Bourret, R.B., Davagnino, J., and Simon, M.I. (1993). The carboxy-terminal portion of the CheA kinase mediates regulation of autophosphorylation by transducer and CheW. J. Bacteriol. *175*, 2097–2101.

Brünger, A.T. (1991). X-PLOR, a System for Crystallography and NMR, Version 3.0 Manual Edition (New Haven, CT: Yale University Press).

Burbulys, D., Trach, K.A., and Hoch, J.A. (1991). The initiation of sporulation in Bacillus subtilis is controlled by a multicomponent phosphorelay. Cell *64*, 545–552.

Chou, K.-C., Maggiora, G.M., Nemethy, G., and Scheraga, H.A. (1988). Energetics of the structure of the four-α-helix bundle in proteins. Proc. Natl. Acad. Sci. USA *85*, 4295–4299.

Collaborative Computational Project, Number 4. (1994). The CCP4 suite: programs for protein crystallography. Acta Crystallogr. D *50*, 760–763.

Connolly, M.L. (1983). Solvent-accessible surfaces of proteins and nucleic acids. Science *221*, 709–713.

Crane, B.R., and Getzoff, E.D. (1997). Determining phases and anomalous scattering factors from the MAD of native protein metal clusters: improved MAD phase error estimates and anomalous scatterer positions. Acta Crystallogr. D *53*, 23–40.

Eisenhaber, F., Persson, B., and Argos, P. (1995). Protein structure prediction: recognition of primary, secondary and tertiary structural features from amino acid sequence. Crit. Rev. Biochem. Mol. Biol. *30*, 1–94.

Fredrick, K.L., and Helmann, J.D. (1994). Dual chemotaxis signaling pathways in Bacillus subtilis: a sigma D-dependent gene encodes a novel protein with both CheW and CheY homologous domains. J. Bacteriol. *176*, 2727–2735.

Furey, W., and Swaminathan, S. (1997). PHASES-95: a program package for processing and analysing diffraction data from macromolecules. Methods Enzymol. *277*, 590–620.

Gegner, J.A., and Dahlquist, F.W. (1991). Signal transduction in bacteria: CheW forms a reversible complex with the protein kinase CheA. Proc. Natl. Acad. Sci. USA *88*, 750–754.

Hess, J.F, Oosawa, K., Kaplan, N., and Simon, M.I. (1988). Phosphorylation of three proteins in the signaling pathway of bacterial chemotaxis. Cell *53*, 79–87.

Holdgate, G.A., Tunnicliffe, A., Ward, W.H., Weston, S.A., Rosenbrock, G., Barth, P.T., Taylor, I.W., Pauptit, R.A., and Timms, D. (1997). The entropic penalty of ordered water accounts for weaker binding of the antibiotic novobiocin to a resistant mutant of DNA gyrase: a thermodynamic and crystallographic study. Biochemistry *36*, 9663–9673.

Holm, L., and Sander, C. (1993). Protein structure comparison by alignment of distance matrices. J. Mol. Biol. *233*, 123–138.

Jackson, A.P., and Maxwell, A. (1993). Identifying the catalytic residue of the ATPase reaction of DNA gyrase. Proc. Natl. Acad. Sci. USA *90*, 11232–11236.

Kato, M., Mizuno, T., Shimizu, T., and Hakoshima, T. (1997). Insights into multistep phosphorelay from the crystal structure of the C-terminal HPt domain of ArcB. Cell *88*, 717–723.

Kishan, K.V.R, Scita, G., Wong, W.T., Di Fiore, P.P., and Newcomer, M.E. (1997). The SH3 domain of Eps8 exists as a novel interwined dimer. Nat. Struct. Biol. *4*, 739–743.

Kofoid, E.C., and Parkinson, J.S. (1988). Transmitter and receiver modules in bacterial signaling proteins. Proc. Natl. Acad. Sci. USA *85*, 4981–4985.

Kraulis, P.J. (1991). Molscript: a program to produce both detailed and schematic plots of protein structures. J. Appl. Crystallogr. *24*, 946–950.

Laskowski, R.A., MacArthur, M.W., Moss, D.S., and Thornton, J.M. (1993). PROCHECK: a program to check the stereochemical quality of protein structures. J. Appl. Crystallogr. *26*, 283–291.

McEvoy, M.M., Hausrath, A.C., Randolph, G.B., Remington, S.J., and Dahlquist, F.W. (1998). Two binding modes reveal flexibility in kinase/response regulator interactions in the bacterial chemotaxis pathway. Proc. Natl. Acad. Sci. USA *95*, 7333–7338.

McRee, D.E. (1992). XtalView: a visual protein crystallographic software system for X11/Xview. J. Mol. Graph. *10*, 44–47.

Merritt, E.A., and Murphy, M.E.P. (1994). Raster3D Version 2.0: a program for photorealistic molecular graphics. Acta Crystallogr. D *50*, 869–873.

Morrison, T.N., and Parkinson, J.S. (1997). A fragment liberated from the *E. coli* kinase that blocks stimulatory, but not inhibitory, chemoreceptor signaling. J. Bacteriol. *179*, 5543–5550.

Oosawa, K., Hess, F.J., and Simon, M.I. (1988). Mutants defective in bacterial chemotaxis show modified protein phosphorylation. Cell *53*, 89–96.

Orengo, C.A., Michie, A.D., Jones, S., Jones, D.T., Swindells, M.B., and Thornton, J.M. (1997). A hierarchic classification of protein domain structure. Structure *5*, 1093–1108.

Otwinowski, A., and Minor, W. (1997). Processing of X-ray diffraction data in oscillation mode. Methods Enzymol. *276*, 307–325.

Panaretou, B., Prodromou, C., Roe, S.M., O'Brien, R., Ladbury, J.E., Piper, P.W., and Pearl, L.H. (1998). ATP binding and hydrolysis are essential to the function of the Hsp90 molecular chaperone in vivo. EMBO J. *17*, 4829–4836.

Park, H., Saha, S.K., and Inouye, M. (1998). Two-domain reconstitution of a functional protein histidine kinase. Proc. Natl. Acad. Sci. USA *95*, 6728–6732.

Parkinson, J.S, and Kofoid, E.C. (1992). Communication modules in bacterial signaling proteins. Annu. Rev. Genet. *26*, 71–112.

Prodromou, C., Roe, S.M., O'Brien, R., Ladbury, J.E., Piper, P.W., and Pearl, L.H. (1997). A molecular clamp in the crystal structure of the N-terminal domain of the yeast Hsp90 chaperone. Cell *90*, 65–75.

Read, R.J. (1986). Improved Fourier coefficients for maps using phases from partial structures with errors. Acta Crystallogr. A *42*, 140–149.

Sander, C., and Schneider, R. (1991). Database of homology-derived protein structures and the structural meaning of sequence alignment. Proteins *9*, 56–68.

Schlessinger, J. (1994). SH2/SH3 signaling proteins. Curr. Opin. Genet. Dev. *4*, 25–30.

Stebbins, C.E., Russo, A.A., Schneider, C., Rosen, N., Hartl, F.U., and Pavlevitch, N.P. (1997). Crystal structure of an Hsp90-Geldamycin complex: targeting of a protein chaperone by an antitumor agent. Cell *89*, 239–250.

Swanson, R.V., Bourret, R.B., and Simon, M.I. (1993a). Intermolecular complementation of the kinase activity of CheA. Mol. Microbiol. *8*, 435–441.

Swanson, R.V., Schuster, S.C., and Simon, M.I. (1993b). Expression of CheA fragments which define domains encoding kinase, phosphotransfer and cheY binding activities. Biochemistry *32*, 7623–7629.

Swanson, R.V., Alex, L.A., and Simon, M.I. (1994). Histidine and aspartate phosphorylation: two-component systems and the limits of homology. Trends Biochem. Sci. *19*, 485–490.

Swanson, R.V., Sanna, M.G., and Simon, M.I. (1996). Thermostable chemotoxis proteins form the hyperthermophilic bacterium *Thermotoga maritima*. J. Bacteriol. *178*, 484–489.

Varughese, K.I., Madhusudan, Zhou, X.Z., Whiteley, J.M., and Hoch, J.A. (1998). Formation of a novel four-helix bundle and molecular recognition sites by dimerization of a response regulator phosphotransferase. Mol. Cell *2*, 485–493.

Welch, M., Chinardet, N., Mourey, L., Birck, C., and Samama, J.P. (1998). Structure of the CheY-binding domain of histidine kinase CheA in complex with CheY. Nat. Struct. Biol. *5*, 25–29.

Wigley, D.B., Davies, G.J., Dodson, E.J., Maxwell, A., and Dodson, G. (1991). Crystal structure of an N-terminal fragment of the DNA gyrase B protein. Nature *351*, 624–629.

Xu, W., Harrison, S.C., and Eck, M.J. (1997). Three-dimensional structure of the tyrosine kinase c-Src. Nature *385*, 595–601.

Yang, Y., and Inouye, M. (1991). Intermolecular complementation between two defective mutant signal-transducing receptors of *E. coli*. Proc. Natl. Acad. Sci. USA *88*, 11057–11061.

Yeh, K.-C., Wu, S.-H., Murphy, J.T., and Lagarias, J.C. (1997). A cyanobacterial phytochrome two-component light sensory system. Science *277*, 1505–1508.

Zhou, H., and Dahlquist, F.W. (1997). Phosphotransfer site of the chemotaxis-specific protein kinase CheA as revealed by NMR. Biochemistry *36*, 699–710.

Zhou, H., Lowry, D.F., Swanson, R.V., Simon, M.I., and Dahlquist, F.W. (1995). NMR studies of the phosphotransfer domain of the histidine kinase CheA from Escherichia coli: assignments, secondary structure, general fold, and backbone dynamics. Biochemistry *34*, 13858–13870.

Brookhaven Protein Data Bank ID Code

Coordinates for CheAΔ289 have been deposited in the Brookhaven Protein Data Bank under ID code 1B3Q.

Note Added in Proof

While this manuscript was under review, the NMR structure of the histidine kinase domain from the class I histidine kinase EnvZ was reported and its similarity to Gyrase B and Hsp90 noted (Tanaka et al. [1998]. NMR structure of the histidine kinase domain of the E. coli osmosensor EnvZ. Nature *396*, 88–92.).